2007 Summer College on Plasma Physics

30 July - 24 August, 2007

**Revised Quantum Electrodynamics
with Fundamental Applications.**

B. Lehnert

*Royal Institute of Technology
Alfven Laboratory
Stockholm, Sweden*

REVISED QUANTUM ELECTRODYNAMICS
WITH FUNDAMENTAL APPLICATIONS

Bo Lehnert

Alfvén Laboratory, Royal Institute of Technology
10044 Stockholm, Sweden
E-mail: Bo.Lehnert@ee.kth.se

Abstract

There are important areas within which conventional electromagnetic theory and its combination with quantum mechanics does not provide fully adequate descriptions of physical reality. These difficulties are not removed by and are not directly associated with quantum mechanics. Instead electromagnetic field theory is a far from completed area of research, and modified forms of it have been elaborated by several investigators during the recent decades. The investigation to be described here has the form of a Lorentz and gauge invariant theory which is based on a nonzero electric field divergence in the vacuum state. It aims beyond Maxwell's equations and leads to new solutions of a number of fundamental problems. The applications include a model of the electron with its point-charge-like nature, the associated self-energy problem, the radial force balance, and a quantized minimum of the elementary electronic charge. There are further applications on the individual photon and on light beams, in respect to the angular momentum (spin), the spatially limited geometry, the associated needle radiation, and the particle-wave nature, such as in the photoelectric effect and in two-slit experiments at low light intensities.

Contents

1 Introduction

Maxwell's equations in the vacuum state have served as guideline and basis in the development of quantum electrodynamics (QED) which has been successful in many applications and has sometimes manifested itself in an extremely good agreement with experiments. However, as pointed out by Feynman [1], there nevertheless exist areas within which conventional electromagnetic theory and its combination with quantum mechanics does not provide fully adequate descriptions of physical reality. These difficulties are not removed by and are not directly associated with quantum mechanics. Instead electromagnetic field theory is a far from completed area of research, and QED will therefore also become subject to the topical shortcomings of such a theory in its conventional form.

As a consequence, modified theories leading beyond Maxwell's equations have been elaborated by several investigators during the recent decades. This advancement of research has been described in books, reviews, and conference proceedings all of which cannot be mentioned here, but where some of the more recent one has been listed in a survey by the author [2].

Among these new approaches there is one theory to be treated in this paper which attaches main importance to conceptual features and leaves out part of the detailed formal deductions which are reported elsewhere [2]–[9]. The theory will be shown to have a number of fundamental applications, such as deduced models of the electron and photon.

2 Some Unsolved Problems in Conventional Theory

There are a number of important physical features which have so far not been fully explained in terms of conventional theory. The first to be mentioned here is the point-charge-like behaviour of the electron which appears to have an extremely small radius. Second, the question arises why the electron does not "explode" under the action of its self-charge. It has been assumed that its internal force balance is due to some unknown nonelectromagnetic cause [10]. Third, the point-charge-like character seems to end up with an infinite self-energy. This problem has been solved in the renormalization procedure by adding extra counter-terms to the Lagrangian, to obtain a finite result from the difference between two infinities. Such a procedure is not quite satisfactory from the physical point of view [11]. Fourth, there is no explanation why the free electronic charge has a quantized minimum value "e", as first shown in the experiments by Millikan.

When further considering the individual photon, it is first noticed that conventional theory does not explain that it has an angular momentum (spin), and this is also the case of a light beam with limited cross-section

[12]. Second, the question arises how a propagating photon can behave as an object with limited spatial extensions, because conventional theory results in divergent solutions and infinite integrals of the field energy when being extended all over space. Third, it still has to be understood how the photon can behave both as a particle and as a wave.

3 Basis of Present Revised Field Equations

To revise the conventional theory we now turn to recent knowledge of and aspects on the vacuum state which is not merely an empty space. Due to quantum mechanics, there is a nonzero level of its ground state, the zero-point energy. Related electromagnetic vacuum fluctuations appear which give rise to the Casimir effect [13] due to which two metal plates attract each other when being brought sufficiently close together. The observed electron-positron pair formation from an energetic photon further demonstrates that electric charges can be created out of an electrically neutral state.

To translate these vacuum properties into a quantitative form, we start with the Lorentz invariant Proca-type field equation in four-space

$$\Box A_\mu \equiv \left(\frac{1}{c^2} \frac{\partial^2}{\partial t^2} - \nabla^2 \right) A_\mu = \mu_0 J_\mu \qquad \mu = 1, 2, 3, 4 \,. \tag{1}$$

Here

$$A_\mu = (\mathbf{A}, i\phi/c) \qquad\qquad J_\mu = (\mathbf{j}, ic\bar{\rho}) \tag{2}$$

with $\mathbf{A}$ and ϕ standing for the magnetic vector potential and the electrostatic potential, and $\mathbf{j}$ and $\bar{\rho}$ representing the three-space current and charge density parts of a general four-current density J_μ constituting the sources of the electromagnetic field. Maxwell's equations in the vacuum are recovered when the four-current density vanishes.

Equations (1) and (2) are now given a new interpretation, where $\bar{\rho}$ is a nonzero charge density which can arise in the vacuum, and $\mathbf{j}$ then stands for an associated current density. Physical experience supports the field equations to remain Lorentz invariant also with this interpretation. It implies that J_μ still has to behave as a four-vector, its square thereby being invariant when transformed from one inertial frame K to another such frame, K'. Thus

$$\mathbf{j}^2 - c^2 \bar{\rho}^2 = \mathbf{j}'^2 - c^2 \bar{\rho}'^2 = 0 \tag{3}$$

if we further require that $\mathbf{j}$ should exist only when there is also a charge density $\bar{\rho}$. This merely becomes analogous to a choice of origin for the space and time coordinates. The final form of the four-current thus becomes

$$J_\mu = \bar{\rho}(\mathbf{C}, ic) \qquad\qquad \mathbf{C}^2 = c^2 \tag{4}$$

where $\mathbf{C}$ is a velocity vector having a modulus equal to the velocity constant c of light. In analogy with the direction to be specified for the current density

in conventional theory, the unit vector $\mathbf{C}/c$ depends on the specific geometry to be considered. There is a connection between the current density (4) and the electron theory by Dirac [5, 8].

The three-dimensional representation of the present revised and extended field equations *in the vacuum* now becomes

$$\text{curl } \mathbf{B}/\mu_0 = \varepsilon_0(\text{div } \mathbf{E})\mathbf{C} + \varepsilon_0 \partial\mathbf{E}/\partial t \tag{5}$$

$$\text{curl } \mathbf{E} = -\partial\mathbf{B}/\partial t \tag{6}$$

$$\mathbf{B} = \text{curl } \mathbf{A} \qquad \text{div } \mathbf{B} = 0 \tag{7}$$

$$\mathbf{E} = -\nabla\phi - \partial\mathbf{A}/\partial t \qquad \text{div } \mathbf{E} = \bar{\rho}/\varepsilon_0 \tag{8}$$

for the electric and magnetic fields $\mathbf{E}$ and $\mathbf{B}$. Here we also include the relation $\text{div } \mathbf{C} = 0$. In these equations there is a dielectric constant ε_0 and a magnetic permeability μ_0 of the conventional vacuum, because they apply to a state which does not include electrically polarized and magnetized atoms or molecules. The new feature of equations (5)–(8) is the appearance of the electric field divergence terms. In principle, a nonzero electric field divergence in the vacuum should not be less conceivable than the nonzero curl of the magnetic field in the vacuum of Maxwell's theory. A nonzero magnetic field divergence is on the other hand not introduced here, but is with Dirac [14] left as an open question as well as that of magnetic monopoles.

Equations (5) and (6) include the field strengths $\mathbf{E}$ and $\mathbf{B}$ only, and are therefore invariant to a gauge transformation. This does not always become the case for equations (1) and (2) when there are other forms of the four-current J_μ.

Using well-known vector identities, equations (5)–(8) result in the local momentum equation

$$\text{div } {}^2\mathbf{S} = \mathbf{f} + \frac{\partial}{\partial t}\mathbf{g} \tag{9}$$

with

$$\mathbf{f} = \bar{\rho}(\mathbf{E} + \mathbf{C} \times \mathbf{B}) \tag{10}$$

$$\mathbf{g} = \varepsilon_0\mathbf{E} \times \mathbf{B} = \frac{1}{c^2}\mathbf{S}. \tag{11}$$

Here ${}^2\mathbf{S}$ is the electromagnetic stress tensor, $\mathbf{f}$ is the volume force density, $\mathbf{g}$ can be interpreted as an electromagnetic momentum density, and $\mathbf{S}$ is the Poynting vector. Likewise a local energy equation

$$-\text{div } \mathbf{S} = \bar{\rho}\,\mathbf{E} \cdot \mathbf{C} + \frac{\partial}{\partial t}w_f \tag{12}$$

is obtained where

$$w_f = \frac{1}{2}\left(\varepsilon_0\mathbf{E}^2 + \mathbf{B}^2/\mu_0\right) \tag{13}$$

3

represents the electromagnetic field energy density. An electromagnetic source energy density

$$w_s = \frac{1}{2}\bar{\rho}\left(\phi + \mathbf{C} \cdot \mathbf{A}\right) \qquad (14)$$

can as well be deduced by recasting the form (13). The volume integrals of w_f and w_s become equal for certain steady configurations which are limited in space [2, 5]. In the cases where the volume force (10) can be neglected, the angular momentum density is finally given by

$$\mathbf{s} = \mathbf{r} \times \mathbf{S}/c^2 \qquad (15)$$

where $\mathbf{r}$ is the radius vector pointing in the direction from the origin.

It has to be remembered that relations (9) and (12) have merely been obtained from a rearrangement of the basic equations. They therefore have forms by which equivalent expressions are obtained for the momentum and energy from the stress tensor.

This section is ended in summarizing the characteristic features of the present revised field equations:

- The theory is based on the pure radiation field in the vacuum state.

- The theory is both Lorentz and gauge invariant.

- The nonzero electric field divergence introduces an additional degree of freedom which changes the character of the field equations substantially, and leads to new physical phenomena.

- The velocity of light is no longer a scalar c but a vector $\mathbf{C}$ which has the modulus c.

4 The Present Form of QED

As shown by Heitler [15] quantization of the electromagnetic field equations, also with included source terms, ends up with the same equations in which the electromagnetic potentials are replaced by their expectation values. In the present approach, which is based on the pure radiation field, a rather good approximation should therefore be obtained in a simplified procedure where relevant quantum conditions are applied afterwards on the general solutions of the field equations. This could be conceived as a way to the most probable state of the quantized solutions.

In the original and current presentation of conventional QED, Maxwell's equations for a vanishing electric field divergence form the basis of the theory [15, 16]. This becomes a further justification for the present theory to use its field equations as a basis for a revised quantum electrodynamic theory.

A special but important question concerns the momentum of the pure radiation field. In conventional QED this momentum is derived from a plane-wave representation and the Poynting vector [15, 16]. In the present theory the Poynting vector and the momentum density (11) have an analogous rôle, in cases where the volume force (10) vanishes or can be neglected.

Here it has also to be noticed that there are nonrelativistic forms in conventional quantum mechanics, such as the Schrödinger equation, in which the quantized momentum has been successfully represented by the operator

$$\mathbf{p} = -i\hbar\nabla \tag{16}$$

for a massive particle. However, this concept leads to some inconsistencies when being applied to a photon model, as discussed later in this context and elsewhere [6].

Thus there are additional points of view which also characterize the present theory:

- Being based on the pure radiation field, the theory includes no ad hoc assumption of particle mass at its outset.

- A possibly arising mass and particle behaviour comes out of "bound" states which result from a type of vortex-like "self-confinement" of the radiation.

- The wave nature results from the "free" states of propagating wave phenomena.

- These "bound" and "free" states can become integrating parts of the same system.

5   Steady Axisymmetric States

Steady electromagnetic field configurations are of special interest, in particular with respect to particles such as the leptons. In contrast to conventional theory, the basic equations (5)–(8) provide a class of steady solutions in the vacuum state. These equations combine to

$$c^2 \operatorname{curl} \operatorname{curl} \mathbf{A} = -\mathbf{C} \left(\nabla^2 \phi \right) = \left(-\bar{\rho}/\varepsilon_0 \right) \mathbf{C} . \tag{17}$$

Here we limit ourselves to particle-shaped states in which the configuration becomes bounded in all spatial directions. In a further restriction to axisymmetry, a spherical frame (r, θ, φ) is introduced in which all quantities are independent of φ. With $\mathbf{C} = (0, 0, C)$, $C = \pm c$, $\mathbf{j} = (0, 0, C\bar{\rho})$, and $\mathbf{A} = (0, 0, A)$, equations (17) reduce to

$$\frac{(r_0\rho)^2 \bar{\rho}}{\varepsilon_0} = D\phi = \left[D + (\sin\theta)^{-2} \right] (CA) \tag{18}$$

where $\rho = r/r_0$ is a dimensionless radial coordinate, r_0 a characteristic radial dimension, $D = D_\rho + D_\theta$ and

$$D_\rho = -\frac{\partial}{\partial \rho}\left(\rho^2 \frac{\partial}{\partial \rho}\right) \qquad D_\theta = -\frac{\partial^2}{\partial \theta^2} - \frac{\cos \theta}{\sin \theta}\frac{\partial}{\partial \theta}. \qquad (19)$$

5.1   The Generating Function

A solution of equation (18) can be obtained in terms of a *generating function*

$$F(r,\theta) = CA - \phi = G_0 \cdot G(\rho,\theta) \qquad (20)$$

where G_0 stands for its characteristic amplitude and G for a normalized dimensionless part. This yields the general solution

$$CA = -(\sin\theta)^2 DF \qquad \phi = -\left[1 + (\sin\theta)^2 D\right]F \qquad (21)$$

$$\bar{\rho} = -\left(\frac{\varepsilon_0}{r_0^2 \rho^2}\right)D\left[1 + (\sin^2\theta)D\right]F. \qquad (22)$$

With the definitions

$$f(\rho,\theta) = -(\sin\theta)D\left[1 + (\sin\theta)^2 D\right]G \qquad (23)$$

$$g(\rho,\theta) = -\left[1 + 2(\sin\theta)^2 D\right]G \qquad (24)$$

the integrated (total) electric charge q_0, magnetic moment M_0, mass m_0, and angular momentum (spin) s_0 then become

$$q_0 = 2\pi\varepsilon_0 r_0 G_0 J_q \qquad I_q = f \qquad (25)$$

$$M_0 = \pi\varepsilon_0 C r_0^2 G_0 J_M \qquad I_M = \rho(\sin\theta)f \qquad (26)$$

$$m_0 = \pi(\varepsilon_0/c^2) r_0 G_0^2 J_m \qquad I_m = fg \qquad (27)$$

$$s_0 = \pi(\varepsilon_0 C/c^2) r_0^2 G_0^2 J_s \qquad I_s = \rho(\sin\theta)fg \qquad (28)$$

where

$$J_k = \int_{\rho_k}^\infty \int_0^\pi I_k \, d\rho d\theta \qquad k = q, M, m, s. \qquad (29)$$

In equation (29) $\rho_k \neq 0$ are small radii of circles being centered around the origin $\rho = 0$ when G is divergent there, and $\rho_k = 0$ when G is convergent at $\rho = 0$. The implication of $\rho_k \neq 0$ will be given later.

A further step is taken by imposing the restriction of a separable generating function

$$G(\rho,\theta) = R(\rho) \cdot T(\theta). \qquad (30)$$

This restriction is useful when treating configurations where the sources $\bar{\rho}$ and $\mathbf{j}$ and the corresponding energy density are mainly localized near the

origin $\rho = 0$, such as for a particle of limited spatial extent [2]. The integrands of the form (29) then become

$$
\begin{align}
I_q &= \tau_0 R + \tau_1 (D_\rho R) + \tau_2 D_\rho (D_\rho R) \tag{31} \\
I_M &= \rho (\sin \theta) I_q \tag{32} \\
I_m &= \tau_0 \tau_3 R^2 + (\tau_0 \tau_4 + \tau_1 \tau_3) R (D_\rho R) + \tau_1 \tau_4 (D_\rho R)^2 + \\
&\quad + \tau_2 \tau_3 R D_\rho (D_\rho R) + \tau_2 \tau_4 (D_\rho R) [D_\rho (D_\rho R)] \tag{33} \\
I_s &= \rho (\sin \theta) I_m \tag{34}
\end{align}
$$

where

$$
\begin{align}
\tau_0 &= -(\sin \theta)(D_\theta T) - (\sin \theta) D_\theta \left[(\sin^2 \theta)(D_\theta T) \right] \tag{35} \\
\tau_1 &= -(\sin \theta) T - (\sin \theta) D_\theta \left[(\sin^2 \theta) T \right] - \sin^3 \theta (D_\theta T) \tag{36} \\
\tau_2 &= -(\sin^3 \theta) T \tag{37} \\
\tau_3 &= -T - 2(\sin^2 \theta)(D_\theta T) \tag{38} \\
\tau_4 &= -2(\sin^2 \theta) T . \tag{39}
\end{align}
$$

5.2 Features of the Generating Function

Among the possible forms to be adopted of the generating function, we will here consider radial parts R which can become convergent or divergent at $\rho = 0$, but which always decrease strongly towards zero when $\rho \to \infty$. The polar part T and its derivatives are always finite. It can be symmetric or antisymmetric with respect to the "equatorial plane" (midplane) defined by $\theta = \pi/2$.

For a radial part R which is convergent at the origin and where $\rho_k = 0$, partial integration yields $J_q = J_{q\rho} J_{q\theta}$ and $J_M = J_{M\rho} J_{M\theta}$ for the integrals (29) where

$$
J_{q\rho} = \int_0^\infty R \, d\rho \qquad J_{M\rho} = \int_0^\infty \rho R \, d\rho \tag{40}
$$

$$
J_{q\theta} = \left\{ (\sin \theta) \frac{d}{d\theta} \left[(\sin \theta)^2 (D_\theta T) \right] + (\sin \theta) \frac{dT}{d\theta} \right\}_0^\pi = 0 \tag{41}
$$

$$
J_{M\theta} = \left\{ (\sin \theta)^3 \frac{d}{d\theta} \left[(\sin \theta)(D_\theta T - 2T) \right] \right\}_0^\pi = 0 . \tag{42}
$$

Thus both q_0 and M_0 vanish in this case.

Concerning the polar part T, the integrals (29) with respect to θ become nonzero for symmetric integrands I_k but vanish for antisymmetric ones. The symmetry or antisymmetry of T further leads to a corresponding symmetry or antisymmetry of $D_\theta T$, $D_\theta \left[(\sin \theta)^2 T \right]$, and $D_\theta \left[(\sin \theta)^2 (D_\theta T) \right]$. As a result the integrated mass m_0 and angular momentum s_0 always become nonzero, whereas the charge q_0 and magnetic moment M_0 have the following features:

7

- A neutral state of vanishing q_0 and M_0 is obtained for a radial part R which is convergent at $\rho = 0$, and regardless of the symmetry properties of the polar function T. This leads to models of the neutrino, not to be treated here in detail but being described elsewhere [2, 6, 8].

- An electrically charged state of nonzero q_0 and M_0 requires a radial part R which is *divergent* at $\rho = 0$, and a polar part T being symmetric with respect to the equatorial plane. At a first glance this appears to lead to divergent final solutions which become physically unacceptable. However, the analysis of the electron model in the following Section 6 demonstrates a way out of this difficulty. It is based on arbitrarily small limits $\rho_k \neq 0$ in equation (29).

5.3   Quantum Conditions of Particle-shaped States

The nonzero electric field divergence provides the field equations with a certain degree of freedom, here manifesting itself in the partly arbitrary form of the generating function. To close the system, relevant quantum conditions have to be imposed, as well as conditions on the force balance which is treated later.

The angular momentum (spin) condition on models of the electron as a fermion, or of the neutrino, is combined with expression (28) to result in

$$s_0 = \pi \left(\varepsilon_0 C / c^2 \right) r_0^2 G_0^2 J_s = \pm h/4\pi \,. \tag{43}$$

This condition is compatible with the two signs of $C = \pm c$ due to relation (4). In particular for a charged particle, equations (25) and (43) combine to a dimensionless charge

$$q^* \equiv |q_0/e| = \left(f_0 J_q^2 / 2 J_s \right)^{1/2} \qquad f_0 = 2\varepsilon_0 ch/e^2 \tag{44}$$

being normalized with respect to the experimentally determined elementary charge "e", and where $f_0 \cong 137.036$ is the inverted value of the fine-structure constant.

According to Dirac [17], Schwinger [18] and Feynman [19] the quantum condition on the magnetic moment of a charged particle such as the electron is determined by

$$M_0 m_0 / q_0 s_0 = 1 + \delta_M \qquad \delta_M = 1/2\pi f_0 \tag{45}$$

which shows excellent agreement with experiments.

Conditions (43) and (45) can also be made plausible by elementary physical arguments based on the present picture of a particle-shaped state of "self-confined" radiation [2, 8].

In a charged particle-shaped state with nonzero magnetic moment, the electric current distribution generates a total magnetic flux Γ_{tot}. The quantized value of the angular momentum s_0 further depends on the type of

configuration to be considered. It becomes $h/4\pi$ for a fermion, but $h/2\pi$ for a boson. Here the electron is conceived to be a system also having a quantized charge q_0. The magnetic flux should then become quantized as well, and be given by the two concepts s_0 and q_0, in a relation having the dimension of magnetic flux. This leads to the flux quantum condition [5, 9]

$$\Gamma_{tot} = |s_0/q_0| \,. \tag{46}$$

6 A Model of the Electron

In this section a model of the electron will be elaborated which in principle also applies to the muon, tauon, and to the corresponding antiparticles.

6.1 The Form of the Generating Function

In accordance with the discussion of Section 5.2, a generating function is now chosen having the parts

$$R = \rho^{-\gamma} e^{-\rho} \qquad \gamma > 0 \tag{47}$$

$$T = 1 + \sum_{\nu=1}^{n} \{a_{2\nu-1} \sin\left[(2\nu - 1)\theta\right] + a_{2\nu} \cos(2\nu\theta)\} \,. \tag{48}$$

Here the radial part R diverges at $\rho = 0$ as required, but the form (47) may at first glance appear to be somewhat special and artificial. Generally one could thus have introduced a negative power series of ρ instead of the single term $\rho^{-\gamma}$. However, due to the analysis which follows, such a series has to be replaced by one single term only, with a locked special value. The exponential factor in expression (47) has further been included to secure convergence of any moment with R at large distances from the origin.

The polar part T represents a general form of geometry having top-bottom symmetry with respect to the equatorial plane.

6.2 Integrated Field Quantities at a Shrinking Characteristic Radius

Since the radial part R is divergent at the origin, its divergence must be outbalanced. This can be done by introducing the concept of a shrinking characteristic radius r_0 to obtain finite integrated field quantities. We therefore define

$$r_0 = c_0 \varepsilon \qquad 0 < \varepsilon \ll 1 \tag{49}$$

where c_0 is a positive constant of the dimension length and ε is a dimensionless smallness parameter. Insertion of the forms (47) and (48) into equations

(25)–(39) yields after some deductions the result

$$q_0 = 2\pi\varepsilon_0 c_0 G_0 \left[J_{q\theta}/(\gamma-1)\right]\left(\varepsilon/\rho_q^{\gamma-1}\right) \tag{50}$$

$$M_0 m_0 = \pi^2(\varepsilon_0^2 C/c^2)c_0^3 G_0^3 \left[J_{M\theta}J_{m\theta}/(\gamma-2)(2\gamma-1)\right]\cdot\left(\varepsilon^3/\rho_M^{\gamma-2}\rho_m^{2\gamma-1}\right) \tag{51}$$

$$s_0 = \pi(\varepsilon_0 C/c^2)c_0^2 G_0^2 \left[J_{s\theta}/2(\gamma-1)\right]\left(\varepsilon/\rho_s^{\gamma-1}\right)^2 \tag{52}$$

where

$$J_{k\theta} = \int_0^\pi I_{k\theta}\,d\theta \qquad k = q, M, m, s \tag{53}$$

is determined from the quantities (35)–(39) and will later be given in its final form. The reason for introducing the compound quantity $M_0 m_0$ in expression (51) is that this quantity appears as a single entity in all finally obtained results of the present theory. A separation of M_0 and m_0 is in itself an important problem which has so far not been considered.

The integrated quantities (50)–(52) are now required to become finite for all values of the parameter ε and of the radii ρ_k, and to scale in such a way that the field geometry becomes independent of ε and ρ_k in the range of small ε. Such a uniform scaling becomes possible when

$$\rho_q = \rho_M = \rho_m = \rho_s = \varepsilon \tag{54}$$

and when the radial parameter γ approaches the value 2 from above, as given by

$$\gamma(\gamma-1) = 2+\delta \qquad 0 \le \delta \ll 1 \qquad \gamma \approx 2+\delta/3\,. \tag{55}$$

From the earlier results (41) and (42) and with relation (55), the integrands $I_{k\theta}$ of equation (53) then reduce to

$$I_{q\theta} = -2\tau_1 + 4\tau_2 \tag{56}$$

$$I_{M\theta}/\delta = (\sin\theta)(-\tau_1 + 4\tau_2) \tag{57}$$

$$I_{m\theta} = \tau_0\tau_3 - 2(\tau_0\tau_4 + \tau_1\tau_3) + 4(\tau_1\tau_4 + \tau_2\tau_3) - 8\tau_2\tau_4 \tag{58}$$

$$I_{s\theta} = (\sin\theta)I_{m\theta}\,. \tag{59}$$

This leads to the finite integrated field quantities

$$q_0 = 2\pi\varepsilon_0 c_0 G_0 A_q \tag{60}$$

$$M_0 m_0 = \pi^2(\varepsilon_0^2 C/c^2)c_0^3 G_0^3 A_M A_m \tag{61}$$

$$s_0 = (1/2)\pi(\varepsilon_0 C/c^2)c_0^2 G_0^2 A_s \tag{62}$$

where

$$A_q \equiv J_{q\theta} \quad A_M \equiv J_{M\theta}/\delta \quad A_m \equiv J_{m\theta} \quad A_s \equiv J_{s\theta} \tag{63}$$

as obtained from equations (53), (55) and (56)–(59).

6.3 The Magnetic Flux

Using equations (21), (19), (47), (49) and (55) the magnetic flux function becomes

$$\Gamma = 2\pi \left(c_0 G_0/C\right) \sin^3 \theta \left[(2 + 2\rho + \rho^2)T - D_\theta T\right] (\varepsilon/\rho). \qquad (64)$$

It increases strongly as ρ decreases towards small values, such as for a point-charge-like behaviour. To obtain a nonzero and finite flux, one has to choose a corresponding dimensionless lower radius limit $\rho = \rho_\Gamma = \varepsilon$, in analogy with relations (49) and (54). There is a main part of the flux the magnetic field lines of which intersect the equatorial plane. This flux is counted from the sphere $\rho_\Gamma = \varepsilon$ and outwards, and is given by

$$\Gamma_0 = -\Gamma(\rho = \varepsilon, \theta = \pi/2) = 2\pi(c_0 G_0/C)A_\Gamma \qquad (65)$$

where

$$A_\Gamma = [D_\theta T - 2T]_{\theta = \pi/2}. \qquad (66)$$

The flux (65) ca be regarded as to be generated by a set of thin current loops which are localized to a spherical surface of radius $\rho = \varepsilon$.

It has to be observed that the flux (65) is not necessarily the total flux generated by the current system as a whole. In the present case it is found that one magnetic island is formed above and one below the equatorial plane, and where each island possesses an isolated flux which does not intersect the same plane [2, 9]. The total flux Γ_{tot} thus consists of the main flux $-\Gamma_0$ plus an extra island flux Γ_i which can be deduced from the function (64).

We now introduce the normalized flux function

$$\Psi \equiv \Gamma(\rho = \varepsilon, \theta)/2\pi(c_0 G_0/C) = \sin^3 \theta(D_\theta T - 2T) \qquad (67)$$

in the upper half-plane if the sphere $\rho = \varepsilon$. The radial magnetic field component vanishes at the angles $\theta = \theta_1$ and $\theta = \theta_2$ in the range $0 \leq \theta \leq \pi/2$. When θ increases from $\theta = 0$ at the axis of symmetry, the flux Ψ first increases to a maximum at the angle $\theta = \theta_1$. Then there follows an interval $\theta_1 \leq \theta \leq \theta_2$ of decreasing flux, down to a minimum at $\theta = \theta_2$. Finally, in the range $\theta_2 \leq \theta \leq \pi/2$ there is again an increasing flux, up to the total main flux value

$$\Psi_0 = \Psi(\pi/2) = A_\Gamma. \qquad (68)$$

This behaviour is due to a magnetic island having dipole-like field geometry with current centra at the angles θ_1 and θ_2 on the spherical surface. We also define the resulting outward island flux

$$\Psi_i = \Psi(\theta_1) - \Psi(\theta_2) \qquad (69)$$

of one magnetic island. The total flux which includes the main flux (68) and that from two magnetic islands then becomes

$$\Psi_{tot} = f_{\Gamma f}\Psi_0 \qquad\qquad f_{\Gamma f} = 1 + 2(\Psi_i/\Psi_0) > 1 \qquad (70)$$

11

where $f_{\Gamma f}$ is a *resulting* flux factor due to the magnetic flied geometry and its magnetic islands.

6.4   The Quantum Conditions

Relevant quantum conditions can now be imposed on the system. For the angular momentum (43) the associated normalized charge (44) becomes

$$q^* = (f_0 A_q^2 / A_s)^{1/2} \,. \tag{71}$$

The magnetic moment relation (45) further reduces to

$$A_M A_m / A_q A_s = 1 + \delta_M \,. \tag{72}$$

Finally the magnetic flux quantization due to condition (46) and expressions (68), (60), (62) and (63) obtains the form

$$8\pi f_{\Gamma q} A_\Gamma A_q = A_s \tag{73}$$

where $f_{\Gamma q}$ is the flux factor being *required* by the quantization. Only when one arrives at a self-consistent solution will the flux factors of equations (70) and (73) become equal to a common factor

$$f_\Gamma = f_{\Gamma f} = f_{\Gamma q} \,. \tag{74}$$

6.5   Variational Analysis on the Integrated Charge

The elementary electronic charge has so far been considered as an independent and fundamental physical constant of nature, determined through measurements only. Since it appears to represent the smallest quantum of free electronic charge, however, the question can be raised whether there is a more profound reason for such a minimum charge to exist.

In the present theoretical approach, standard variational analysis was first applied to the normalized charge (71), including Lagrange multipliers when treating relations (72) and (73) as subsidiary conditions, and having the amplitudes $a_{2\nu-1}$ and $a_{2\nu}$ of the expansion (48) as independent variables. This attempt failed, because there was no well-defined extremum point in amplitude space but instead a clearly expressed plateau behaviour. The analysis then proceeded by successively including an increasing number of amplitudes which are "swept" (scanned) across their entire range of variation [9]. The results were as follows:

- In the case of four amplitudes (a_1, a_2, a_3, a_4) the normalized charge q^* was found to behave as shown in Fig. 1. Here conditions (72) and (73) have been imposed with a_3 and a_4 being left as variables for the scanning. There is a steep barrier of large q^* for values of a_3 and a_4
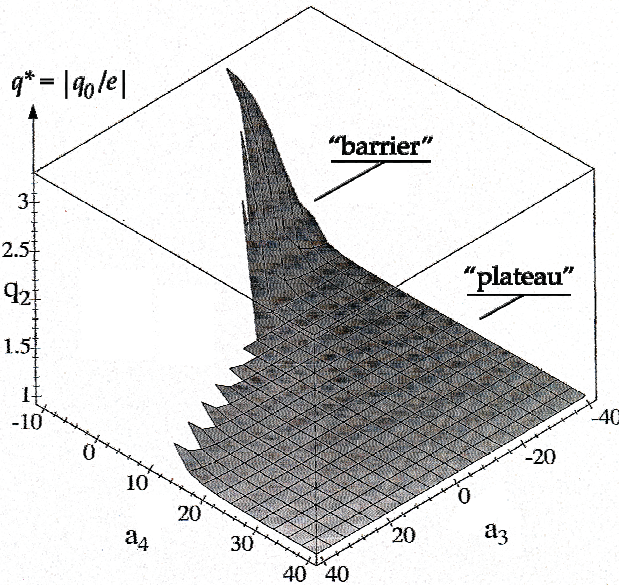
Figure 1: The normalized electron charge $q^* \equiv |q_0/e|$ as a function of the two amplitudes a_3 and a_4, for solutions satisfying the subsidiary quantum conditions for a fixed flux factor $f_\Gamma = f_{\Gamma q} = 1.82$, and being based on a polar function T having four amplitudes (a_1, a_2, a_3, a_4). The deviations of this profile from that obtained for the self-consistent solutions which obey condition (74) are hardly visible on the scale of the figure.

near the origin, and a very flat "plateau" close to the experimental value $q^* = 1$ in the ranges of large $|a_3|$ and $a_4 > 0$. This plateau is slightly "warped", having values which vary along its perimeter from $q^* = 0.969$ with $f_\Gamma = 1.81$ to $q^* = 1.03$ with $f_\Gamma = 1.69$.

- At an increasing number of amplitudes beyond four, there is a similar but slightly changed and somewhat higher plateau. This can be understood in the way that the contributions in the expansion (48) from higher order multipoles should have a limited effect on the integrated profiles of the polar function T. Moreover, an increase of the minimum level of q^* at the inclusion of an extra variable is not in conflict with the variational principle, because any function can have minima when some of its included variables vanish. Thus the four-amplitude case appears to be that which ends up with the lowest value of q^*.

6.6 The Radial Force Balance

The outcome of the variational analysis with its plateau behaviour still includes some remaining degree of freedom to be investigated. In a steady state equation (9) shows that the total acting forces can be represented by the volume force density (10). The latter only consists of an electrostatic force due to the electron charge in conventional theory, and this tends to "explode" the electron [10, 20]. In the present theory, however, there is an extra magnetic force which under certain conditions can outbalance the electrostatic one, at least when being integrated over the entire volume. A local balance defined by $\mathbf{f} = 0$ does on the other hand not seem to be possible, because this leads to an overdetermined system of equations.

In a straight circular geometry of constant charge density, limited radius and with an axial velocity vector, the radial force (10) vanishes [2]. A local balance can on the other hand not be fully realized in the present geometry, but the integrated radial force can in any case be made to vanish. Thus, with the results obtained from equations (18)–(22) and (30), an integrated radial force

$$F_r = -2\pi\varepsilon_0 G_0^2 \iint \left[DG + D\left(s^2 DG\right)\right] \cdot \left[\frac{\partial G}{\partial \rho} - \frac{1}{\rho}s^2 DG\right]\rho^2 s\, d\rho d\theta \quad (75)$$

is obtained where $s = \sin\theta$ and

$$\rho^2 DG = D_\theta T - 2T \quad (76)$$

in the present point-charge-like model. The force balance (75) has the form

$$F_r = I_+ - I_- \quad (77)$$

where I_+ is a positive radially outward directed contribution due to the electrostatic part of the volume force, and I_- is a negative negative inward directed (confining) contribution due to its magnetic part. Thus $I_+/I_- = 1$ defines an integrated radial force balance. When applied to the four-amplitude case for Fig. 1, the values of the normalized charge q^* and the related values of the ratio I_+/I_- are found to vary along the perimeter of the plateau. The integrated force ratio decreases from $I_+/I_- = 1.27$ at $q^* = 0.98$ to $I_+/I_- = 0.37$ at $q^* = 1.01$, thus passing an equilibrium point $I_+/I_- = 1$ at $q^* \cong 0.988$. The remaining degrees of freedom of this case have then been used up.

To sum up, a combination of a lowest possible normalized charge q^* with the requirement of an integrated radial force balance results in a value $q^* \cong 0.988$ which deviates only by one percent from the experimental value of the elementary free charge. The reason for this small deviation is not clear at this stage. One possible explanation could be due to a necessary small quantum mechanical correction of the magnetic flux, in analogy with that

of the magnetic moment in equation (45). Another possibility may be due to a small error resulting from the large number of steps to be performed in numerical analysis which includes matching of the quantum conditions (71)–(73), of the flux factors (74), and of the contributions (77) to the radial force balance.

7 Models of the Photon

In a model of the individual photon as a propagating boson, a wave or wave packet with preserved and limited geometrical shape as well as with undamped motion in a defined direction, has to be taken as a starting point. This leads to cylindrical waves in a frame (r, φ, z) , with z in the direction of propagation. As in conventional theory, an initial arbitrary disturbance can in principle be represented by a spectrum of plane waves with normals in different directions, but would then become disintegrated at later times [20]. In this revised analysis we further introduce a velocity vector

$$\mathbf{C} = c(0, \cos \alpha, \sin \alpha) \tag{78}$$

of helical geometry where the angle α is constant and

$$0 < \cos \alpha \ll 1 \tag{79}$$

for reasons to be clarified later. In fact, $\cos \alpha$ and $\sin \alpha$ can have either sign, as determined by the two directions of spin and propagation, but are here restricted to positive values for the sake of simplicity.

The basic equations (5)–(8) can be combined to the wave equation

$$\left(\frac{\partial^2}{\partial t^2} - c^2 \nabla^2 \right) \mathbf{E} + \left(c^2 \nabla + \mathbf{C} \frac{\partial}{\partial t} \right) (\operatorname{div} \mathbf{E}) = 0 \,. \tag{80}$$

of the electric field, and further in a cylindrical frame to

$$\left(D_1 - \frac{1}{r^2} + \frac{1}{r^2} \frac{\partial^2}{\partial \varphi^2} \right) E_r - \frac{2}{r^2} \frac{\partial}{\partial \varphi} E_\varphi = \frac{\partial}{\partial r} (\operatorname{div} \mathbf{E}) \tag{81}$$

$$\left(D_1 - \frac{1}{r^2} + \frac{1}{r^2} \frac{\partial^2}{\partial \varphi^2} \right) E_\varphi + \frac{2}{r^2} \frac{\partial}{\partial \varphi} E_r = \left[\frac{1}{r} \frac{\partial}{\partial \varphi} + \frac{1}{c} \left(\cos \alpha \right) \frac{\partial}{\partial t} \right] (\operatorname{div} \mathbf{E}) \tag{82}$$

$$\left(D_1 + \frac{1}{r^2} \frac{\partial^2}{\partial \varphi^2} \right) E_z = \left[\frac{\partial}{\partial z} + \frac{1}{c} \left(\sin \alpha \right) \frac{\partial}{\partial t} \right] (\operatorname{div} \mathbf{E}) \tag{83}$$

where

$$D_1 = \frac{\partial^2}{\partial r^2} + \frac{1}{r} \frac{\partial}{\partial r} + \frac{\partial^2}{\partial z^2} - \frac{1}{c^2} \frac{\partial^2}{\partial t^2} \,. \tag{84}$$

A divergence operation on equation (5) yields

$$\left[\frac{\partial}{\partial t} + c(\cos \alpha) \frac{1}{r} \frac{\partial}{\partial \varphi} + c(\sin \alpha) \frac{\partial}{\partial z} \right] (\operatorname{div} \mathbf{E}) = 0 \tag{85}$$

when div $\mathbf{C} = 0$. Equation (85) sometimes becomes useful, but it does not introduce more information than that already contained in equation (80). In the present theory where div $\mathbf{E} \neq 0$ the symmetry between the fields $\mathbf{E}$ and $\mathbf{B}$ has been broken. The magnetic field has instead to be given by the electric field through the induction law (6).

In a normal mode analysis every field quantity Q is here represented by the form

$$Q = Q(\rho) \exp\left[i(-\omega t + \bar{m}\varphi + kz)\right] \equiv Q(\rho) \exp(i\theta_m) \qquad (86)$$

where $\rho = r/r_0$, ω is the angular frequency, and k the axial wave number. In connection with the operator (84) and the form (86) we further define

$$K_0^2 = (\omega/c)^2 - k^2 \, . \qquad (87)$$

7.1 Conventional Wave Modes

In conventional theory div $\mathbf{E}$ drops out of equations (5)–(8) and (81)–(83). The condition of a vanishing electric field divergence can be taken implicitly into account by introducing the Herz vector [20]. For $K_0^2 > 0$ the phase velocity ω/k becomes larger and the group velocity $\partial\omega/\partial k$ smaller than c, as obtained from relation (87). The general solution then has field components in terms of Bessel functions $Z_{\bar{m}}(K_0 r)$ of the first and second kind, where the r-dependence of every component is of the form $Z_{\bar{m}}/r$ or $Z_{\bar{m}+1}$ [20]. These solutions can be applied to wave guides with boundary conditions given by surrounding metal walls. Application of the same solutions, as well as of those for any value of K_0^2 to a model of an individual photon with angular momentum (spin) leads on the other hand to physically irrelevant results:

- Already the special purely axisymmetric case $\bar{m} = 0$ results in $s_z = 0$ due to equation (15), and thus in zero spin.

- The photon model cannot be bounded by walls but has to concern the entire surrounding vacuum space. But then the total integrated field energy becomes divergent. This also applies to an attempt to form a wave packet for each of the field components.

Consequently, conventional theory based on Maxwell's equations does not lead to a physically acceptable photon model.

7.2 Axisymmetric Space-charge Wave Modes

As a next step equations (81)–(85) are applied to purely axisymmetric space-charge waves where $\partial/\partial\varphi = 0$ but div $\mathbf{E} \neq 0$. Equation (85) then results in the dispersion relation

$$\omega = kv \qquad v = c(\sin\alpha) \qquad (88)$$

16

which has phase and group velocities both being equal to v for a constant value of α. Combination of equations (81), (88) and (82) then yields

$$ik(\cos\alpha)^2 E_r = \frac{\partial E_z}{\partial r} \tag{89}$$

and

$$\left(D - \frac{1}{\rho^2}\right) E_\varphi = -(\mathrm{tg}\alpha)DE_z \tag{90}$$

where

$$D = \bar{D}_\rho - \bar{\theta}^2(\cos\alpha)^2\,, \qquad \bar{D}_\rho = \frac{\partial^2}{\partial\rho^2} + \frac{1}{\rho}\frac{\partial}{\partial\rho}\,, \qquad \bar{\theta} = kr_0\,. \tag{91}$$

Here a *generating function*

$$G_0 \cdot G = E_z + (\cot\alpha)E_\varphi \qquad G = R(\rho)e^{i(-\omega t + kz)} \tag{92}$$

can be found which combines with equations (89)–(91) and (6) to the field components

$$E_r = -iG_0\left[\theta(\cos\alpha)^2\right]^{-1}\frac{\partial}{\partial\rho}\left[\left(1 - \rho^2 D\right)G\right] \tag{93}$$

$$E_\varphi = G_0\left(\mathrm{tg}\,\alpha\right)\rho^2 DG \tag{94}$$

$$E_z = G_0\left(1 - \rho^2 D\right)G \tag{95}$$

and

$$B_r = -G_0\left[c(\cos\alpha)\right]^{-1}\rho^2 DG \tag{96}$$

$$B_\varphi = -iG_0(\sin\alpha)\left[\theta c(\cos\alpha)^2\right]^{-1}\frac{\partial}{\partial\rho}\left[\left(1 - \rho^2 D\right)G\right] \tag{97}$$

$$B_z = -iG_0\left[\theta c(\cos\alpha)\right]^{-1}\left(\frac{\partial}{\partial\rho} + \frac{1}{\rho}\right)(\rho^2 DG)\,. \tag{98}$$

These solutions give rise to a nonzero spin. By a proper choice of the generating function the integrated field energy also becomes finite.

With the dispersion relation (88) it is seen that condition (79) has to be satisfied for the group velocity not to get in conflict with experiments of the Michelson-Morley type. For $\cos\alpha \leq 10^{-4}$ the deviation of this velocity from c would thus become less than a change in the eight decimal of c.

We are free to rewrite the amplitude factor of the generating function (92) as

$$G_0 = g_0(\cos\alpha)^2\,. \tag{99}$$

With this notation and the solutions (93)–(98), the components E_r and B_φ are of zero order in the smallness parameter $\cos\alpha$, E_φ, B_r and B_z of first

order, and E_z of second order. There is thus essentially a radially polarized cylindrical wave.

A wave packet can be formed from the normal mode solutions, having a narrow line width, as required from experiments and observations, and with the spectral amplitude distribution

$$A_k = \left(\frac{k}{k_0^2}\right) \exp\left[-z_0^2 (k - k_0)^2\right] \tag{100}$$

where k_0 is the main wave number, $2z_0$ represents the axial packet length, and $k_0 z_0 \gg 1$ in the narrow line limit. Integration over the spectrum is performed with the notation $\bar{z} = z - vt$ and

$$\bar{E}_0 = E_0(\bar{z}) = \left(\frac{g_0}{k_0 r_0}\right) \left(\frac{\sqrt{\pi}}{k_0 z_0}\right) \exp\left[-\left(\frac{\bar{z}}{2z_0}\right)^2 + ik_0\bar{z}\right]. \tag{101}$$

It results in the average packet field components

$$\bar{E}_r = -iE_0 \left[R_5 + (\theta_0')^2 R_1\right] \tag{102}$$

$$\bar{E}_\varphi = E_0\theta_0(\sin\alpha)(\cos\alpha) \left[R_3 - (\theta_0')^2 R_1\right] \tag{103}$$

$$\bar{E}_z = E_0\theta_0(\cos^2\alpha) \left[R_4 + (\theta_0')^2 R_1\right] \tag{104}$$

$$\bar{B}_r = -\left(\frac{1}{c}\right)(\sin\alpha)^{-1} E_\varphi \tag{105}$$

$$\bar{B}_\varphi = \left(\frac{1}{c}\right)(\sin\alpha) E_r \tag{106}$$

$$\bar{B}_z = -i\left(\frac{1}{c}\right) E_0(\cos\alpha)[R_8 - (\theta_0')^2 R_7] \tag{107}$$

where

$$R_1 = \rho^2 R \qquad R_2 = dR_1/d\varphi \qquad R_3 = \rho^2 \bar{D}_\rho R \tag{108}$$

$$R_4 = R - R_3 \qquad R_5 = dR_4/d\rho \qquad R_6 = \bar{D}_\rho R_4 \tag{109}$$

$$R_7 = \left(\frac{d}{d\rho} + \frac{1}{\rho}\right) R_1 \qquad R_8 = \left(\frac{d}{d\rho} + \frac{1}{\rho}\right) R_3. \tag{110}$$

Since expressions (105)–(107) have been obtained in the narrow-line approximation, the condition div $\mathbf{B} = 0$ is only satisfied approximately, whereas it holds exactly for the normal mode solutions (96)–(98).

In the following analysis a generating function is chosen which is symmetric with respect to the axial centre $\bar{z} = 0$ of the moving wave packet. Then

$$G = R(\rho)\cos k\bar{z} \tag{111}$$

when the real parts of (92) and (101) are adopted. Here G and (E_φ, E_z, B_r) are symmetric and (E_r, B_φ, B_z) are antisymmetric functions of z with respect to $\bar{z} = 0$.

18

The analysis now proceeds in forming the spatially integrated average field quantities which represent an electric charge q, magnetic moment M, total mass m, and spin s. The limits of z are $\pm\infty$, and those of ρ will later be specified. The integrated charge becomes

$$q = 2\pi\varepsilon_0 \int \left\{ \frac{\partial}{\partial r}(r^2 \int_{-\infty}^{+\infty} \bar{E}_r d\bar{z}) + r[\bar{E}_z]_{-\infty}^{+\infty} \right\} dr = 0 \qquad (112)$$

and the integrated magnetic moment

$$M = \pi\varepsilon_0 c(\cos\alpha) \int \left\{ r\frac{\partial}{\partial r}(r \int_{-\infty}^{+\infty} \bar{E}_r d\bar{z}) + r^2[\bar{E}_z]_{-\infty}^{+\infty} \right\} dr = 0 \qquad (113)$$

due to the symmetry properties of the field components. It should be observed that, even if q and M vanish, the local charge density and magnetic field strength are nonzero.

For the total mass the Einstein relation yields

$$m = \left(\frac{1}{c^2}\right) \int w_f \, dV \qquad (114)$$

with dV as a volume element and the field energy density given by equation (13). Using equations (102)–(107) and the energy relation by Planck, the narrow-line limit then gives the result

$$m \cong 2\pi \left(\varepsilon_0/c^2\right) \int_{-\infty}^{+\infty} \int r|\bar{E}_r^2| \, dr d\bar{z} = a_0 W_m = h\nu_0/c^2 \,. \qquad (115)$$

Here $\nu_0 = c/\lambda_0$ is the average frequency related to the average wave length $\lambda_0 = 2\pi/k_0$ of the packet,

$$a_0 = \varepsilon_0 \pi^{5/2} \sqrt{2} z_0 \left(g_0/ck_0 z_0\right)^2 \equiv 2a_0^* g_0^2 \qquad (116)$$

and

$$W_m = \int \rho R_5^2 \, d\rho \,. \qquad (117)$$

The slightly reduced phase and group velocity of equation (88) becomes associated with a very small nonzero rest mass

$$m_0 = m \left[1 - (v/c)^2\right]^{1/2} = m(\cos\alpha) \,. \qquad (118)$$

This can be further verified [2], by comparing the total energy of the wave packet in the laboratory frame K with that in a frame K' following the packet motion at the velocity $c(\sin\alpha) < c$ of equation (88).

Turning to the integrated angular momentum, we first notice that the volume force (10) contains the vector $\mathbf{E} + \mathbf{C} \times \mathbf{B}$. From equations (78) and (102)–(107) is readily seen that the volume force has a vanishing component

19

$\bar{f}_\varphi$ and that its components $\bar{f}_r$ and $\bar{f}_z$ are of second order in the smallness parameter $\cos\alpha$. Consequently, and somewhat in analogy with the force balance of the electron in Section 6.6, there is here a local transverse force balance, as provided by a confining magnetic force contribution.

The density of angular momentum (15) in the axial direction now becomes

$$\bar{s}_z = \varepsilon_0 r(\bar{E}_z \bar{B}_r - \bar{E}_r \bar{B}_z) \cong -\varepsilon_0 r \bar{E}_r \bar{B}_z \tag{119}$$

which is on the other hand of first order in $\cos\alpha$. Consequently, the volume force can be neglected and the contribution from the momentum density (11) due to the Poynting vector dominates the right hand member of the momentum equation (9). The total spin becomes

$$s = \int \bar{s}_z \, dV = a_0 r_0 c (\cos\alpha) W_s = h/2\pi \tag{120}$$

for the photon as a boson, and where

$$W_s = -\int \rho^2 R_5 R_7 \, \mathrm{d}\rho. \tag{121}$$

The results (120) and (118) show that a nonzero spin s requires a nonzero rest mass m_0 to exist. These two concepts are associated with the component C_φ of the velocity vector. This component circulates around the axis of symmetry and has two opposite possible spin directions.

To proceed further the radial function $R(\rho)$ has to be specified. A form

$$R(\rho) = \rho^\gamma \mathrm{e}^{-\rho} \qquad \gamma > 0 \tag{122}$$

being convergent at $\rho = 0$ is first considered. It has a maximum at the radius $\hat{r} = \gamma r_0$ and drops rapidly towards zero at large ρ. When evaluating the integrals (117) and (121), the Euler integral

$$J_{2\gamma-2} = \int_0^\infty \rho^{2\gamma-2} e^{-2\rho} \, d\rho = 2^{-(2\gamma+3)} \Gamma(2\gamma+1) \tag{123}$$

appears in terms of the gamma function. For $\gamma \gg 1$ only the dominant terms prevail, and the result becomes

$$W_m = 2^{-(2\gamma+4)} \gamma^6 (2\gamma-1)\Gamma(2\gamma+1) = W_s/\gamma. \tag{124}$$

Combination of relations (115), (120) and (124) finally leads to an effective photon diameter

$$2\hat{r} = \frac{\lambda_0}{\pi(\cos\alpha)} \tag{125}$$

being independent of γ and of the exponential factor in equation (122), The diameter (125) is limited but large as compared to atomic dimensions when the wave length λ_0 is in the visible range.

20

We next turn to a radial function

$$R(\rho) = \rho^{-\gamma}\mathrm{e}^{-\rho} \qquad\qquad \gamma > 0 \qquad\qquad (126)$$

which *diverges* at the axis. Here $\hat{r} = r_0$ can be taken as an effective radius. This situation becomes similar to that of the electron model in Section 6.1 and a discussion of its radial form will not be repeated. To obtain finite integrated values of the total mass m and spin s, small lower radial limits ρ_m and ρ_s are introduced in the integrals (117) and (121). We further make the Ansatz

$$r_0 = c_r \cdot \varepsilon \qquad g_0 = c_g \cdot \varepsilon^{\beta} \qquad 0 < \varepsilon \ll 1 \qquad\qquad (127)$$

of shrinking values for both the characteristic radius and the amplitude of the generating function, and where c_r, c_g and β are positive constants. Equations (115) and (120) combine to

$$m = a_0^* \gamma^5 c_g^2 \left(\varepsilon^{2\beta}/\rho_m^{2\gamma} \right) \cong h/\lambda_0 c \qquad\qquad (128)$$

$$s = a_0^* \gamma^5 c_g^2 c_r c (\cos\alpha) \left(\varepsilon^{2\beta+1}/\rho_m^{2\gamma-1} \right) = h/2\pi \, . \qquad\qquad (129)$$

To obtain finite m and s it is then necessary that

$$\rho_m = \varepsilon^{\beta/\gamma} \qquad\qquad \rho_s = \varepsilon^{(2\beta+1)(2\gamma-1)} \, . \qquad\qquad (130)$$

We are here free to choose $\beta = \gamma \gg 1$ by which $\rho_s \cong \rho_m = \varepsilon$. This leads to a similar set of geometrical configurations in the range of small ε. Combination of equations (128) and (129) yields an effective photon diameter

$$2r_0 = \frac{\varepsilon\lambda_0}{\pi(\cos\alpha)} \qquad\qquad (131)$$

being independent of γ and β. Here ε and $\varepsilon/(\cos\alpha)$ can be made small enough to result in "needle radiation" at a diameter (131) which becomes comparable to atomic dimensions.

The obtained results (125) and (131) of an axisymmetric photon model can be illustrated by a simple example where $\cos\alpha = 10^{-4}$. For a wave length $\lambda_0 = 3 \times 10^{-7}$ m equation (125) yields a photon diameter of about 10^{-3} m, and equation (131) results in a diameter smaller than 10^{-7} m when $\varepsilon < \cos\alpha$ for needle-like radiation.

The individual photon models resulting from the present theory appear to be relevant in respect to the particle-wave dualism. A subdivision into a "bound" particle part associated with the component C_φ and a "free" pilot wave part associated with the component C_z is imaginable but not necessary. This is because the rest mass here merely constitutes an integrating part of the total field and its energy. In other words, the wave packet behaves as an entirety, having particle and wave properties at the same time. Such a

21

joint particle-wave nature of the single individual photon reveals itself in the comparatively small effective radius, especially in the case of a needle-like shape. This is reconcilable with the photoelectric effect where a photon knocks out an electron from an atom, and also with the dot-shaped marks which form an interference pattern on a screen in two-slit experiments at low light intensity [21], as well as with recent such experiments under different boundary conditions [22]. Thereby the interference patterns should also arise in the case of cylindrical waves. The nonzero rest mass may further make it possible for the photon to perform spontaneous transitions between different wave modes, by means of proposed "photon oscillations" [2, 4, 6], in analogy with the neutrino oscillations.

7.3 Screw-shaped Space-charge Wave Modes

In a review by Battersby [23] twisted light is described where the energy travels along cork-screw-shaped paths. This discovery is expected to become important in communication and microbiology.

Corresponding modes should exist in the present theory for a nonzero $\bar{m}$ in equations (81)–(85). As compared to the purely axisymmetric normal modes, these screw-shaped modes lead to a more complex analysis, partly on account of the second term in equation (5). In a first iteration we attempt to neglect this term due to its small factor $\cos\alpha$, and then end up again with the dispersion relation (88). From equation (83) the component E_z is seen to be of the order $(\cos\alpha)^2$ as compared to E_r and E_φ. Thereby equation (81) would take the form

$$E_r \cong -\left(\frac{r}{\bar{m}}\right)\left[1 - k^2(\cos\alpha)^2\left(\frac{r}{\bar{m}}\right)^2\right]\left(\frac{\partial}{\partial r} + \frac{1}{r}\right)(iE_\varphi). \tag{132}$$

When inserting this relation into equation (82), the latter becomes identically satisfied up to first order in $\cos\alpha$. Consequently the component iE_φ can be used in this approximation as a generating function

$$iE_\varphi = F = G_0 G, \qquad G = R(\rho)\exp(i\theta_m). \tag{133}$$

In analogy with the deductions in Section 7.2, wave packet solutions can be formed, q and M be found to vanish, the volume force (10) to be neglected in equation (9), and expressions for m and s to be obtained [4]. With the same convergent radial function as in equation (122), there is a nearly radially polarized wave in which

$$|\bar{E}_r/i\bar{E}_\varphi| = |\gamma + 1 - \rho| \gg 1 \tag{134}$$

for $\rho \ll \gamma$ and $\gamma \gg 1$. Moreover, insertion of E_r from expression (132) into equation (83) shows that E_φ and E_z are of the same order in the parameter

γ. Thus equation (134) shows that also $|E_r/iE_z| \gg 1$. The effective photon diameter would then become

$$2\hat{r} = \frac{\lambda_0 \bar{m}^{3/2}}{\pi(\cos\alpha)} \qquad\qquad \bar{m} \neq 0\,. \qquad (135)$$

However, this result is not fully consistent with the basic equations. Relation (88) and insertion of $r = \hat{r}$ from equation (135) namely shows that the second term in equation (85) is of second order in $\cos\alpha$ as well as the sum of its other two terms. To remove this difficulty, the analysis has to be restricted to configurations where R is peaked at a nearly constant value of r, to form a ring-shaped radial distribution. This is in fact what happens with the form (122) which becomes strongly peaked at $\hat{r} = \gamma r_0$ in the limit of large γ.

As a next "iteration" we therefore replace the variable r in the second term of equation (85) by a constant value

$$\bar{r} = \bar{m}^{3/2}/c_1 k(\cos\alpha) \qquad (136)$$

where c_1 is a positive constant. This implies that the dispersion relation is modified to

$$k^2 - (\omega/c)^2 \cong k^2(\cos\alpha)^2 C_0 \qquad C_0 = 1 - 2c_1/\sqrt{\bar{m}}\,. \qquad (137)$$

As a result, the effective photon diameter becomes

$$2\hat{r} = \frac{\lambda_0 \bar{m}^{3/2}}{\pi(\cos\alpha)\sqrt{C_0}} \qquad\qquad \bar{m} \neq 0\,. \qquad (138)$$

This result is consistent with expression (136) for $r = \hat{r}$, provided that

$$C_0 = 1 + (2/\bar{m}) - (2/\bar{m})\sqrt{(1/\bar{m}) + 1} \qquad (139)$$

where one solution has been discarded because c_1 and C_0 have to be positive. The value of $\sqrt{C_0}$ ranges from 0.414 for $\bar{m} = 1$ to 1 for large values of $\bar{m}$.

The result (138) as well as those of equations (125) and (131) are applicable both to individual photons and to dense light beams of N photons per unit length, because the corresponding integrated mass and angular momentum both become proportional to N. In the beam case, the effective diameters then stand for those of the corresponding beam models. This also applies to the present screw-shaped mode with a convergent and ring-shaped radial part of the generating function which seems to be consistent with experimental observations [23]. Here screw-shaped normal modes of radii (138) with slightly different values of $\cos\alpha$ can be superimposed to form a ring-shaped beam profile of a certain width.

Attempts to analyze screw-shaped modes having a divergent radial part R and aiming at a needle-shaped behaviour are faced with the difficulties of equation (85) when the configuration extends all the way to the axis.

8 The Linearly Polarized Photon Beam

The photon and beam models studied here have so far essentially been radially polarized. We now turn to the case of a linearly polarized light beam of circular cross section. Elliptically or circularly polarized beams are obtained from the superposition of linearly polarized modes being ninety degrees out of phase. For linear polarization a rectangular frame of reference would become suitable, whereas a cylindrical one becomes preferable for a circular cross-section.

Without changing the essential features the analysis is simplified by the restriction to a homogeneous core with plane wave geometry, limited radially by a narrow boundary region in which the light intensity drops to zero. The radius of the beam is large as compared to the characteristic wave length, and the boundary conditions can in a first approximation be applied separately to every small local segment of the boundary. A localized analysis is then performed in which the electric field vector of the core wave forms a certain angle with the boundary, and where local rectangular coordinates can be introduced. In its turn, the core wave is then subdivided into two waves of the same frequency and wavelength, but having electric field vectors being perpendicular and parallel to the local segment of the boundary region.

8.1 Flat-shaped Beam Geometry

In the analysis on a segment of the boundary region, a local frame (x, y, z) is now chosen with z in the axial direction of propagation, and with the normal of the boundary in the x-direction. There is no y-dependence. The velocity vector is given by

$$\mathbf{C} = c(0, \cos\alpha, \sin\alpha) \qquad 0 < \cos\alpha \ll 1 \qquad (140)$$

thus having C_y along the boundary and C_z in the direction of propagation. From a divergence operation on equation (5), a dispersion relation of the form (88) is again obtained. The wave equation (80) for normal modes now reduces to the three relations

$$E_x = -\left[\frac{i}{k(\cos\alpha)^2}\right]\frac{\partial E_x}{\partial x} \qquad (141)$$

$$\left[k^2(\cos\alpha)^2 - \frac{\partial^2}{\partial x^2}\right]E_y - ik(\cos\alpha)(\sin\alpha)\left(\frac{\partial E_x}{\partial x} + ikE_z\right) = 0 \quad (142)$$

$$\frac{\partial E_x}{\partial x} = -\left[\frac{i}{k(\cos\alpha)^2}\right]\frac{\partial^2 E_z}{\partial x^2} \qquad (143)$$

where relation (143) is merely obtained from derivation of (141). Combination of equations (141) and (142) gives

$$\left[k^2(\cos\alpha)^2 - \frac{\partial^2}{\partial x^2}\right]\left(E_y + \frac{\sin\alpha}{\cos\alpha}E_z\right) = 0. \qquad (144)$$

Equations (141) and (144) thus show that the component E_z can serve as a generating function for the transverse components E_x and E_y. At least one solution of equation (144) is readily found when E_y and E_z have the same spatial profiles and

$$E_y = -\frac{\sin\alpha}{\cos\alpha}E_z \tag{145}$$

The ordering of the electric field components with respect to the smallness parameter $\cos\alpha$ is thus $E_x = O(1)$, $E_y = O(\cos\alpha)$ and $E_z = O(\cos^2\alpha)$.

The magnetic field components are finally given by

$$\omega(B_x, B_y, B_z) = \left(-kE_y, kE_x + i\frac{\partial E_z}{\partial x}, -i\frac{\partial E_y}{\partial x}\right) \tag{146}$$

From relation (88) we have

$$B_x = -E_y/c(\sin\alpha) \tag{147}$$

$$B_y = E_x/c(\sin\alpha) + \frac{i}{kc(\sin\alpha)}\frac{\partial E_z}{\partial x} = (\sin\alpha)E_x/c \tag{148}$$

$$B_z = -\frac{i}{kc(\sin\alpha)}\frac{\partial E_y}{\partial x} = -(\cos\alpha)E_x/c \tag{149}$$

where $B_x = O(\cos\alpha)$, $B_y = O(1)$ and $B_z = O(\cos\alpha)$.

Application of relations (88) and (145) on the result (147)–(149) finally yields

$$\mathbf{E} + \mathbf{C} \times \mathbf{B} = 0\,. \tag{150}$$

This implies that the volume force (10) vanishes identically in rectangular geometry, and the Poynting vector is again the source of the electromagnetic momentum.

8.2 Two Special Flat-shaped Cases

Two special plane cases are now studied of a beam which has a core region defined by $-a < x < a$ and two narrow boundary regions $-b < x < -a$ and $a < x < b$ of the small thickness $d = b - a$. There is symmetry in respect to $x = 0$ and we discuss only the region at $x = a$ henceforth. With the chosen frame there is first the case in which E_x is the main component. Within the core region a homogeneous linearly polarized plane wave is assumed to exist, having the constant components E_{x0} and B_{y0}.

Inside the boundary region an axial field E_z is assumed to increase linearly with x from a small value near $x = a$, and in such a way that E_x in equation (141) becomes matched to E_{x0} at $x = a$. Within the same region E_z further passes a maximum, after which it drops to zero at the edge $x = b$. There is then a reversed field E_x in the outer part of the boundary layer, and the maximum strength of E_x is of the same order as E_{x0} according to equation (141). From equation (145) the spatial profile of E_y further becomes

the same as that for E_z. The component B_y of equation (148) is matched to B_{y0} at the edge of the core region and to lowest order in $\cos\alpha$. Then the Poynting vector components become $S_x = 0$ and

$$S_y \cong -E_x B_z/\mu_0 = c(\cos\alpha)\varepsilon_0 E_x^2 \qquad (151)$$

$$S_z \cong E_x B_y/\mu_0 = c(\sin\alpha)\varepsilon_0 E_x^2. \qquad (152)$$

Thus there is a primary flow S_z of momentum in the direction of propagation, a secondary flow S_y along the boundary, and no flux S_x across it. The field energy density (13) becomes

$$w_f \cong \varepsilon_0 E_x^2 \qquad (153)$$

to lowest order in $\cos\alpha$.

Turning then to the second case where E_y is the main field component, being parallel with the boundary, there is a plane wave in the core region with the components E_{y0} and B_{x0}.

Within the boundary region, in a small range of x near $x = a$, the axial field E_z is now assumed to be constant, and E_x thus vanishes due to equation (141). Then relation (145) makes it possible to match E_y to E_{y0} at $x = a$. The field E_z is further chosen to decrease towards zero when approaching the outer edge $x = b$. According to equations (141) and (145) this results in a perpendicular field component

$$E_x = \left[\frac{i}{k(\cos\alpha)(\sin\alpha)}\right]\frac{\partial E_y}{\partial x} \qquad (154)$$

which first reaches a maximum and then drops to zero at $x = b$. For a characteristic length L_{cy} of the derivative of E_y the ratio

$$|E_x/E_y| = \lambda/2\pi L_{cy}(\cos\alpha) \qquad (155)$$

can then become smaller than unity. Thus with $\lambda/L_{cy} = 10^{-4}$ and $\cos\alpha = 10^{-4}$ this ratio is about 0.16. The magnetic field components (147)–(149) now have the ordering $|B_x| = O(1) > |B_y|$ and $B_z = O(\cos\alpha)$ when E_x is smaller than E_y. Here B_x can be matched to B_{x0} at $x = a$, since both B_y and E_x vanish at $x = a$ due to equation (148). The Poynting vector components finally become $S_x = 0$ and

$$S_y = c(\cos\alpha)\varepsilon_0 E_y^2 \left[1 + (\sin\alpha)^2(E_x/E_y)^2\right]/(\sin\alpha)^2 \qquad (156)$$

$$S_z = c\varepsilon_0 E_y^2 \left[1 + (\sin\alpha)^2(E_x/E_y)^2\right]/(\sin\alpha)^2. \qquad (157)$$

Also here the flow of momentum is essentially of the same character as in the first case. The field energy density becomes

$$w_f \cong \varepsilon_0 E_y^2 \qquad (158)$$

as long as $E_x^2 \ll E_y^2$.

8.3 The Plane Core Wave

There is an additional problem with the matching of the solutions at the edge of the beam core. This is due to the fact that the phase and group velocity of expression (88) for the present electromagnetic space-charge (EMS) wave in the boundary region is slightly smaller than that of a conventional plane electromagnetic (EM) wave in the core. However, this problem can be solved by introducing a plane EMS wave in the core which becomes hardly distinguishable from a plane EM core wave.

We start with the basic equations (5)–(8) for a plane wave where all quantities vary as

$$Q = Q_0 \exp\left[i(-\omega t + \mathbf{k} \cdot \mathbf{r})\right] \tag{159}$$

and Q_0 is a constant. For the velocity vector we now use the form

$$\mathbf{C} = c\left[(\cos\beta)(\cos\alpha), (\sin\beta)(\cos\alpha), \sin\alpha\right] . \tag{160}$$

From the last of equations (8) the dispersion relation (88) is then recovered, and a matching of the phase velocity becomes possible. The basic equations further result in

$$c^2 k(-B_y, B_x) = \left[(kE_z)C_x - \omega E_x, (kE_z)C_y - \omega E_y\right] \tag{161}$$

$$c(\sin\alpha)(B_x, B_y) = (-E_y, E_x) \tag{162}$$

and $B_z = 0$. Combination of equations (161) and (162) yields

$$E_z(C_x, C_y) = -(\cos\alpha)^2 c(E_x, E_y) \tag{163}$$

and

$$E_x/E_y = C_x/C_y = (\cos\beta)/(\sin\beta) . \tag{164}$$

Here E_z is small due to equation (163). The first flat-shaped case corresponds to the choice of a small $\sin\beta$, whereas the second one is represented by a small $\cos\beta$. In this way a plane EMS wave is obtained which differs very little from a plane EM wave, with the exception of the phase velocity which now can be matched to that of the wave in the boundary region. A matching of the field components can be made as in Section 8.2.

8.4 Simplified Analysis on the Spin of a Circular Beam

The results of the analysis on the small segments of the circular perimeter are now put together to form a first simplified approach to a circular beam in a frame (x, y, z), thus consisting of a homogeneous field $\mathbf{E}_0 = (E_0, 0, 0)$ and $\mathbf{B}_0 = (0, B_0, 0)$ in its core, and with a narrow boundary layer with large derivatives. Introducing the angle φ between the y-direction and the radial direction counted from the axis, the electric field components of the core are expressed by

$$E_{0\perp} = E_0 \sin\varphi \qquad E_{0\parallel} = E_0 \cos\varphi \tag{165}$$

27

in the perpendicular and parallel directions of the boundary.

In the boundary region $\mathbf{E}^2 = E_0^2$ at the edge of the core. With the restriction $E_x^2 \ll E_y^2$ in expressions (155)–(157), the contributions (151) and (156) to the Poynting vector add up in the transverse direction along the boundary to

$$S_t = c(\cos \alpha)\varepsilon_0 \mathbf{E}^2 \tag{166}$$

being independent of the angle φ. The energy density of the beam core can further be written as

$$w_{fc} = \varepsilon E_0^2 = n_p hc/\lambda \tag{167}$$

where n_p is the number of equivalent photons per unit volume. With a parallel spin $h/2\pi$ of each photon, the core would possess a total equivalent (imagined) angular momentum per unit length

$$s_c = r_0^2 n_p h/2 = \varepsilon_0 E_0^2 \lambda r_0^2/2c \tag{168}$$

as obtained from combination with equation (167), and with r_0 standing for the radius of the core. Due to equations (166) and (15) the real angular momentum generated per unit axial length in the boundary layer becomes on the other hand

$$s_b = 2\pi(\cos \alpha)\varepsilon E_0^2 f_E r_0^2 d/c \tag{169}$$

where $d \ll r_0$ is the thickness of the layer and $f_E < 1$ is a profile factor of order unity obtained from integration of $\mathbf{E}^2$ over the same layer. This yields the ratio

$$\frac{s_b}{s_c} = \frac{4\pi(\cos \alpha)f_E d}{\lambda} . \tag{170}$$

For the equivalent angular momentum s_c of the core to be replaced by a real angular momentum s_b being generated in the boundary layer, the result thus becomes $s_b = s_c$ or

$$d = \frac{\lambda}{4\pi f_E(\cos \alpha)} \tag{171}$$

which is analogous to the effective photon diameter relation (125) in the case of a convergent radial part of the generating function (92). As an example, $\lambda = 3 \times 10^{-7}$ m, $f_E = 0.2$ and $\cos \alpha = 10^{-4}$ leads to a physically relevant value of $d \cong 10^{-3}$ m for a beam with a radius $r_0 = 10^{-2}$ m, say.

It should be observed that equation (168) applies to a case where all imagined core photons have spin in the same axial direction. There is also an imagined situation where two unequal fractions of the photons could have opposite spin directions. This still results in a net beam angular momentum as observed in experiments [12, 15], but requiring a smaller layer thickness (171) at given values of the remaining parameters. In this consideration it should also be remembered that a plane wave does not give rise to a spin.

We finally notice that the obtained results should also hold for a corresponding field configuration in the limit of a single photon model. Such a

photon could thus become linearly polarized in its "core", and be limited in the transverse direction by an outer "mantle" of radially decreasing field intensity within which an angular momentum is being generated.

9 Comments on the Momentum of the Radiation Field

The pure radiation field has a momentum density $\mathbf{g}$ being based on equations (9)–(11) and the Poynting vector. The latter has also been used as a basis for the conventional and original QED theory described by Schiff [16] and Heitler [15] among others.

In the case of a massive particle, the quantized momentum has on the other hand been represented successfully by the operator $\mathbf{p}$ of expression (16) in the nonrelativistic Schrödinger equation [16]. For the normal wave modes (86) treated in this context the corresponding axial component becomes

$$p_z = \hbar k = h/\lambda = h\nu/c. \tag{172}$$

In conventional theory this component is related to a photon of energy $h\nu$, moving along z at the velocity c of light.

A comparison between the concepts of $\mathbf{g}$ and $\mathbf{p}$ leads, however, to a number of not quite clear questions concerning $\mathbf{p}$. These are as follows:

- In the present theory based on the concept of $\mathbf{g}$, individual photons as well as light beams are limited spatially in the directions being perpendicular to the axial direction of propagation and have vanishing or negligible transverse losses of momentum. This is not the case when applying the concept $\mathbf{p}$ which has a radial component and leads to a corresponding transverse loss, thus becoming questionable from the physical point of view.

- In a pure axisymmetric case the concept $\mathbf{g}$ results in a momentum directed around the axis of symmetry. The same momentum vanishes when applying the concept $\mathbf{p}$.

- In the present Lorentz invariant photon model the momentum $\mathbf{g}$ has a component around the axis which provides a spin at the expense of the axial velocity of propagation which becomes slightly reduced below c. With the concept $\mathbf{p}$ the result (172) is in conventional theory indicating that the photon moves at the full velocity c in the axial direction. But for the same photon to possess a nonzero spin, there should also exist an additional transverse momentum p_φ corresponding to an additional velocity v_φ which circulates around the z axis. However, this would lead to a superlumial total velocity within the photon configuration.

10   Conclusions

In the present revised quantum electrodynamic theory, the nonzero electric field divergence introduces an additional degree of freedom and modifies the basic field equations to a considerable extent, thereby also giving rise to new results and interpretations in respect to a number of fundamental applications.

Considering the resulting models of leptons such as the electron, the field equations contain additional electric field divergence terms which constitute large contributions already at the outset, and which give rise to a number of new features:

- The point-charge behaviour comes out as a necessity from the theory, with the requirement of a nonzero net electric charge.

- The infinite self-energy problem of the point charge is eliminated in the present theory in which a divergent behaviour of the generating function is outbalanced by a shrinking characteristic radius. This provides a physically more acceptable and realistic alternative to the renormalization process in which extra ad hoc counter terms are merely added to the Lagrangian, to outbalance one infinity by another.

- The integrated electrostatic force of the electron configuration can be outbalanced by an integrated magnetic force. This prevents the electron from "exploding" under the action of its self-charge. This so far not understood balance can be conceived as a kind of electromagnetic confinement.

- Variational analysis, in combination with the requirement of an integrated electromagnetic force equilibrium, leads to a deduced and quantized elementary charge which deviates by only one percent from its experimental value. If this small deviation could be understood and removed, the electronic charge would no longer remain an independent constant of nature, but become deduced from the velocity of light, Planck's constant, and the dielectric constant.

In the applications to photon and light beam physics, the nonzero electric field divergence appears at a first sight as a small quantity, but it still comes out to have essential effects on the end results:

- The theory leads to a spin of the individual photon, not being obtained from conventional theory in a physically relevant field configuration. The present cylindrical field geometry is helical.

- It is explained how a propagating photon can behave as an object of limited spatial extensions, and even in the form of needle radiation,

whereas conventional theory results in solutions which are extended over space and lead to a divergent integrated field energy.

- The individual photon wave packet solutions have simultaneous particle and wave properties. They become reconcilable both with the photoelectric effect and with the dot-shaped marks and their interference patterns in two-slit experiments at low light intensities.

- There is electromagnetic confinement of the local transverse forces in a propagating photon wave packet, somewhat in analogy with that of the electron.

- Also a photon beam of limited cross-section has a spin which can be explained by the present theory, and not by conventional analysis.

- The observed ring-shaped intensity profile of screw-shaped light beams is consistent with the present theory.

References

[1] Feynman,R.P., *Lectures in Physics: Mainly Electromagnetism and Matter*, Addison-Wesley, Reading, Massachusetts, 1964.

[2] Lehnert,B., International Review of Electrical Engineering (I.R.E.E.), *1*, n.4(2006)452; Royal Institute of Technology, Stockholm, Report TRITA-ALF-2004-02, 2004.

[3] Lehnert,B., Speculations in Science and Technology, *9*(1986)117.

[4] Lehnert,B., Physica Scripta *T82*(1999)89; *66*(2002)105; *T113*(2004)41; *72*(2005)359; *74*(2006)139.

[5] Lehnert,B., *Modern Nonlinear Optics* (M. W.Evans, I. Prigogine, S. A. Rice, Editors), Vol.*119*, PartII,1, John Wiley and Sons, Inc., New York, 2001.

[6] Lehnert,B., Progress in Physics, *2*(2006)78; *3*(2006)43; *1*(2007)1.

[7] Lehnert,B., *Dirac Equation, Neutrinos and Beyond* (V.V.Dvoeglazov, Editor), Ukrainian Journal: Electromagnetic Phenomena, T.3, No1(9), (2003)35.

[8] Lehnert,B. and Roy,S., *Extended Electromagnetic Theory*, World Scientific Publishers, Singapore, 1998.

[9] Lehnert,B. and Scheffel,J., Physica Scripta, *65*(2002)200.

[10] Jackson,J.D., *Classical Electrodynamics*, John Wiley and Sons, Inc., New York, 1962, Ch. 17.4, p.589.

[11] Ryder,L.H., *Quantum Field Theory*, Cambridge Univ. Press, 1996, Ch.9.3, p.321; see also edition of 1987.

[12] Ditchburn,R.W., *Light*, Academic Press, London, 1976, Third Edition, Sec.17.24.

[13] Casimir,H.B.G., Proc.K.Ned.Akad.Wet. *51*(1948)793.

[14] Dirac,P.A.M., *Directions in Physics*, Wiley-Interscience, New York, 1978.

[15] Heitler,W., *The Quantum Theory of Radiation*, Third Edition, Clarendon Press, Oxford, 1954, p.409; Ch.II.

[16] Schiff,L.I., *Quantum Mechanics*, McGraw-Hill Book Comp.,Inc., New York, 1949, Ch.XIV, Ch.II.

[17] Dirac,P.A.M., Proc.Roy.Soc. *117*(1928)610 and *118*(1928)351.

[18] Schwinger,J., Phys.Rev. *76*(1949)790.

[19] Feynman,R.P., *QED: The strange theory of light and matter*, Penguin, London, 1990.

[20] Stratton,J.A., *Electromagnetic Theory*, McGraw-Hill Book Comp., New York and London, 1941, Ch.II, Sec.2.5; Ch.VI, Sec.6.7.

[21] Tsuchiya,T., Inuzuka,E., Kurono,T., and Hosada,M., Advances in Electronics and Electron Physics, *64A*(1985)21.

[22] Afshar,S.S., Flores,E., McDonald,K.F., and Knoesel,E., Foundations of Physics, *37*(2007)295.

[23] Battersby,S., New Scientist, 12 June 2004, p.37.